CUTTING TEST AS A SOURCE OF FRACTURE TOUGHNESS AND SHEAR YIELD STRENGTH FOR AXIAL-PERPENDICULAR MODEL OF WOOD CUTTING

*Lud'ka Hlásková**

Assistant Professor
E-mail: ludka.hlaskova@mendelu.cz

Zdeněk Kopecký

Associate Professor
E-mail: zdenek.kopecky@mendelu.cz

Aleš Solař

Assistant Professor
Department of Wood Processing Technologies
E-mail: ales.solar@mendelu.cz

Zdeněk Patočka

Assistant Professor
Department of Forest Management and Applied Geoinformatics
Mendel University in Brno
Brno, Czech Republic
E-mail: zdenek.patocka@mendelu.cz

(Received July 2018)

Abstract. The objective of this study was to develop and design a model of calculation of fracture parameters for axial–perpendicular direction of wood cutting. Two selected wood species of Central Europe provenance spruce (*Picea abies* L.) and beech (*Fagus sylvatica* L.) of two different levels of MC ($w = 8\%$ and 16%) were sawn. Measurements of energetic effects (cutting power and cutting force) while sawing wood were carried out on the laboratory stand, simulating conditions of circular saw blade cutting. Using the newly designed model, it is possible to determine fracture toughness and shear yield strength only on the basis of the cutting tests. Unknown parameters, which are then applied in the model, were set based on calculation of the forces acting on the workpiece and the tool. Using the measured cutting force and the feed force, other components of the resulting active force were calculated. The computation was based on Ernst–Merchant's force decomposition diagram. Results confirmed the obvious influence of the anatomical structures and MC on the size of fracture parameters.

Keywords: Fracture toughness, shear yield strength, wood cutting, circular saw blade, cutting test.

INTRODUCTION

The question of whether fracture and crack propagation play a role in the cutting process has a complex history. According to Patel et al (2009), Reuleaux (1990) was the first to deal with this issue. Williams (1998), Atkins (2003), Laternser et al (2003), and Williams et al (2010) dedicated several scientific studies to understanding how cutting forces are involved in cutting by linking this process to fracture mechanics. On the basis of the performed experiments, Atkins (2005) has suggested that the forces involved in the cutting process depend not only on the cutting edge geometry and on the basic properties of the material, but also, to a large extent, on fracture mechanics–related processes. This approach shows that the cutting forces depend both on toughness of the material and on plasticity and friction, which fact offers a methodology suitable for determining

* Corresponding author

toughness and deformation stress from the performed experiments for a number of solid substances, including metals, plastics, and wood (Orlowski and Palubicki 2009). The main parameters of the model, using fracture mechanics, are shear yield strength τ and fracture toughness R (Atkins 2005). The new computational model further uses the application of Ernst–Merchant's theory for wood cutting by a saw blade. Atkins (2003, 2005, 2009), applying the original Ernst–Merchant equation and his own experiments, has developed an equation of forces involved in the cutting process. Based on the Ernst–Merchant diagram, magnitudes of the forces acting on the workpiece and on the tool are calculated (Kopecký et al 2014). With the application of the results based on fracture tests, further progress can be made by analyzing the cutting process. Fracture is an important parameter in all machining processes (Atkins 2003; Atkins 2005). Kowaluk (2007) applied the results obtained during longitudinal cutting and wood milling and also fracture mechanics to chipboard machining (Kowaluk et al 2004). Wyeth et al (2009) used Atkins' theory (Atkins 2003; Atkins 2009) for two classical cases of orthogonal wood cutting, where the first is type I chip formation, which is commonly called the chip that is formed by bending (Franz 1958; Williams 1998), and the second is the type II chip that forms by shearing.

The main objective of this article was to develop and design a new model of calculation of fracture parameters for axial-perpendicular direction of wood cutting that would allow simplification and refinement. Using the newly designed model, it is possible to determine fracture toughness and shear yield strength only on the basis of the cutting tests without performing complex fracture tests.

Theoretical Background

The cutting kinematics (Fig 1) makes it clear that the saw blade teeth move at the constant cutting velocity v_c along a circular trajectory. When cutting, this rotating movement compounds with the linear workpiece movement v_f, ie the tooth cutting edge moves along a cycloid. Furthermore, it is difficult to assume that under this kind of sawing kinematics, there is a case of perpendicular cutting because the angle between the grains and the cutting speed direction differs from 90° ($\varphi_3 = 0$-90°), as it was assumed for the sash gang saw and the band sawing machines. The rotation movement of the cutting tool and the steady feed result in the change in chip thickness. The model of the main edge of the tooth is axial-perpendicular toward the grain direction (∥–⊥), with $\varphi_1 = 90°$, $\varphi_2 = 0°$-90°, and $\varphi_3 = 0°$-90°.

When calculating, the mean uncut chip thickness h_m is considered; it is determined at the point of the mean fiber cutting angle φ_2. From the

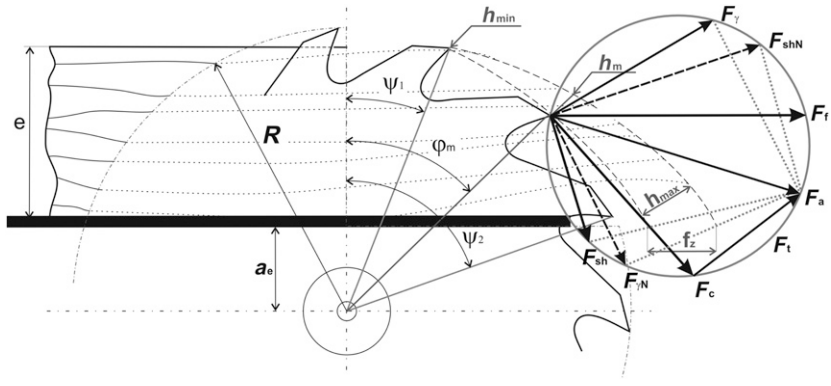

Figure 1. Ernst–Merchant's diagram: F_c, cutting force; F_t, thrust force; F_{sh}, the force required to shear the wood along the shear plane; F_{shN}, normal force on the shear plane; F_γ, friction force on the rake face; $F_{\gamma N}$, normal force to the rake face; F_f, feed force; F_a, active force.

geometry of circular saw blade cutting, it is evident that the angle of fiber cutting varies. At the point of tooth contact with the workpiece, it equals to the entry angle ψ_1, which is given by $\psi_1 = \arccos\left(\frac{a_e + e}{R}\right)$; at the point of circular saw blade teeth disengagement, it equals to the exit angle ψ_2, which can be determined as $\psi_2 = \arccos\left(\frac{a_e}{R}\right)$, where R is the circular saw blade radius, e is the workpiece height, and a_e is the position of the workpiece. The mean fiber cutting angle φ_2 is then determined as the average value of both angles. When the tooth begins to cut, the uncut chip thickness has the minimum $h_{\min}$ value. The maximum uncut chip thickness $h_{\max}$ is reached at the moment when the tooth leaves the workpiece. As already mentioned, the mean uncut chip thickness h_m is considered in the calculation models.

The mean uncut chip thickness is then calculated from the following relationship:

$$h_m = f_z \cdot \sin \varphi_2 \tag{1}$$

According to the latest theoretical knowledge using fracture mechanics methods (Atkins 2003; Orlowski 2007; Orlowski et al 2013), the mathematical model of power calculation for circular saw blade cutting can be expressed in the following form:

$$\begin{aligned} P_c &= F_c \cdot v_c + P_{ac} \\ &= \left[z_a \cdot \frac{\tau_{\gamma\parallel\perp} \cdot b \cdot \gamma}{Q_{shear}} h_m \cdot v_c + z_a \cdot \frac{R_{\parallel\perp} \cdot b}{Q_{shear}} \cdot v_c \right] + \dot{m} \cdot v_c^2, \end{aligned} \tag{2}$$

where z_a is the number of simultaneously cutting teeth, $\tau_{\gamma\parallel\perp}$ is the shear yield strength, b is the saw kerf width, γ is the shear strain along the shear plane, h_m is the mean uncut chip thickness, v_c is the cutting speed, $R_{\parallel\perp}$ is the specific work of surface separation (fracture toughness), Q_{shear} is the friction correction coefficient, and $\dot{m}$ is the mass flow of chips.

The terms in Eq 2 express the power necessary for chip bending and cutting, the power to overcome friction between the workpiece and the tool blade, and the power necessary for surface separation. The term after the bracket does not express the force ratios during chip separation itself but expresses the kinetic energy for chip removal by the circular saw blade. All this work is provided externally from the cutting force components moving in parallel to the machined surface. This means that it affects only the total consumed saw power (Orlowski et al 2013).

The following is valid for the chip mass flow:

$$\dot{m} = \frac{b \cdot l \cdot v_f \cdot \rho_w}{2}, \tag{3}$$

where b is the saw kerf width, l is the cut length, v_f is the feed speed, and ρ_w is the wood density.

It is important to pinpoint that this model assumes perfect sharpness of the cutting edge. Moreover, it does not consider the effect of blunting and chip momentum because of the mean values of feed speeds during wood cutting.

Unknown parameters of the model were calculated, based on calculation of the forces acting on the workpiece and the tool (Fig 1). Using the measured cutting force F_c and the feed force F_f, other components of the resulting active force were calculated—the computation was based on Ernst–Merchant's diagram. First of all, the shear plane angle Φ was determined. For large uncut chip thicknesses (for which the shear plane angle Φ is constant), the Ernst–Merchant equation can serve as the basis:

$$\Phi = \left(\frac{\pi}{4}\right) - \left(\frac{1}{2}\right)\left(\beta_\mu - \gamma_f\right), \tag{4}$$

where β_μ is the friction angle given by $\tan^{-1}\mu = \beta_\mu$, μ is the coefficient of friction, and γ_f is the rake angle.

Using the shear plane angle, the shear strain along the shear plane γ can be calculated from the equation:

$$\gamma = \frac{\cos\gamma_f}{\cos\left(\Phi - \gamma_f\right)\sin\Phi}. \tag{5}$$

The friction correction coefficient Q_{shear} is calculated according to the following formula:

$$Q_{\text{shear}} = \left[1 - \sin\beta_{\mu} \cdot \sin\Phi / \left(\cos\left(\beta - \gamma_{\text{f}}\right)\cos\left(\Phi - \gamma_{\text{f}}\right)\right)\right] \quad (6)$$

The friction correction coefficient Q_{shear} depends in principle on the orientation of the shear plane to the machined surface. If the shear plane angle Φ equals to zero (the tool does not cut the chip), the friction correction coefficient Q_{shear} is constant and equals to 1 (see Eq 6).

If chips are formed by shearing, the cutting force size can be established experimentally. The relationship between the cutting force and the uncut chip thickness is considered linear when cutting most of the materials. The only exception is the zone of extremely thin chips, when the cutting mechanism changes significantly. The same results are reported by Csanády and Magoss (2013) for processing wood and wood-based materials. This conclusion was confirmed experimentally for frame saw (Orlowski 2007; Orlowski and Atkins 2007; Orlowski and Palubicki 2009) and for circular saw cutting (Kopecký et al 2014; Hlásková et al 2015). This is why it is possible to describe precisely the dependence of the cutting force on the varying uncut chip thickness, using two experimental points resulting from at least two independent measurements. The cutting force, related to one tooth, is in the model, using fracture mechanics, expressed by the line slope.

From the measured data, a graph of dependence of the cutting force per one tooth F_{c}^{1z} on the uncut chip thickness h_{m} was created. The data points were intersected by a line (linear trendline), and the regression equation was obtained (see Fig 2):

Regression equation is in the form:

$$F_{\text{c}}^{1z} = \left(\frac{\tau_{\gamma\parallel\perp} \cdot b \cdot \gamma}{Q_{\text{shear}}}\right) \cdot h_m + \left(\frac{R_{\parallel\perp} \cdot b}{Q_{\text{shear}}}\right) \quad (7)$$

The shear yield strength is determined from the slope of the linear regression line:

$$\tau_{\gamma\parallel\perp} = \frac{k \cdot Q_{\text{shear}}}{b \cdot \gamma} \quad (8)$$

This part of the energy is used to create the chip and represents the energy necessary for plastic deformation of the unit material volume. The slope of the linear regression line k, therefore, reflects consumption of the energy for chip formation and for its permanent strain.

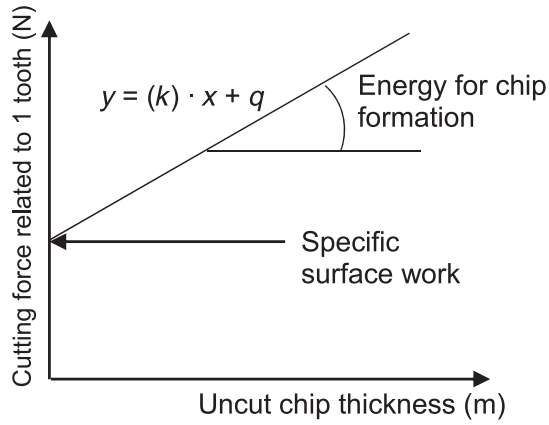

Figure 2. Linear trendline.

$$R_{\parallel\perp} = \frac{q \cdot Q_{\text{shear}}}{b} \quad (9)$$

MATERIALS AND METHODS

Experimental Device

Measurements were performed on the test bench simulating conditions of circular saw cutting in real operation as accurately as possible (Kopecký and Rousek 2012). The stand is based on a fixed stator of the DC dynamometer of DS 442-2/V model. The speed of the spindle, on which the saw blade is mounted, can be controlled continuously by the Leonard device up to n = 12,000 rpm at a maximum torque of M_{c} = 14 N·m. The material is fixed on a movable carriage, which is led toward the cut in linear guides and is fed by a ball screw. The screw is driven by an asynchronous electric motor via a frequency converter, controlling material feed toward the cutting unit. The feed speed can be changed in the range v_{f} = 3-22 m·min^{-1}.

Measurement of the torque M_{c} and the rotational speed n is performed, using the T34 FN-HBM contactless sensor. It consists of two basic parts: a rotor and a stator. The T34 FN-HBM sensor is

connected, via the connectors, with the Spider8 measuring control unit, which feeds and at the same time processes the output torque *Mc* and the rotational speed n signals. The control unit communicates with the computer, where the control software assesses the processed signal. Spider8 is an electronic measuring system designed for measuring mechanical quantities (force, pressure, travel, speed, relative elongation, etc) through the connected sensors (passive or active).

The workpiece feed force is measured tensiometrically by the S2-HBM resistive dynamometer (HBM, Darmstadt, Germany), which senses tension and pressure up to 100 N or 200 N, with the class of accuracy of 0.05. The dynamometer is located between the ball screw nut and the infeed carriage in such a way that its torsional stress, which would cause measurement inaccuracies, may be avoided.

Circular Saw Blade

The circular saw blade for longitudinal wood cutting, manufactured by the company Flury Systems AG (Arch, Switzerland), was used for the experiment. It is a standard blade with straight teeth. In the cutting zone of the blade, four radial expansion grooves, ended by a copper rivet compensating corrugation because of increasing temperature and reduced noise level, are burned in. Moreover, this blade has a modified tension by rolling. Design parameters of the circular saw blade were as follows: diameter $D = 350$ mm, teeth number $z = 28$, hole diameter $d = 30$ mm, saw blade thickness $s = 2.5$ mm, tooth height $h = 10.5$ mm, clearance angle $\alpha_f = 15°$, and rake angle $\gamma_f = 20°$. The saw blade was clamped with collars 100 mm in diameter.

Material

Beech wood (*Fagus silvatica* L.) and spruce wood (*Picea abies* L.) samples originating from the Training Forest Enterprise Masaryk Forest Křtiny, an organizational part of Mendel University in Brno, Czech Republic, were used. The length of specimens used for the experiment was 800 mm. The thickness of the samples was $e = 21$ mm. The width of the samples was 500 mm; however, because of the manner in which the tests were conducted, these parameters were insignificant. Moisture was detected by a wood moisture meter (HMB-WS25; Merlin Technology GmbH, Tumeltsham, Austria), which was used for quick nondestructive wood moisture measurements. The gravimetric method was used to more accurately determine the moisture of the samples. Additional information on materials (average moisture and density value) can be found in Table 1.

Cutting Conditions

Feed speed was changed in the range $v_f = 2$-22 $m \cdot min^{-1}$ with the step shown in Table 2. This corresponded to the changing mean uncut chip thickness h_m. For the present cutting conditions, a series of measurements, subject to statistical assessment, was performed. Twenty-five measurements were made for each feed speed. Variation coefficient of the torque was approximately 3.6% and of the feed force was 4.8%, indicating low data variability.

Calculation of the kinematic elements of circular saw cutting was performed in accordance with the aforementioned relations. These variables are the input parameters for calculation of the fracture parameters.

RESULTS AND DISCUSSION

The torque and feed force curves are shown in Fig 3, where it is possible to distinguish three phases of cutting. At the beginning of the process of cutting, the torque and the feed force rise steeply and reach the maximum value, with stabilization afterward. This part of the record is the most important because we can determine the actual

Table 1. Additional information on cutting conditions and materials.

	Beech8	Beech16	Spruce8	Spruce16
w (%)	8.1	16.2	8.2	16.1
ρ_w ($kg \cdot m^{-3}$)	761	768	420	429

Table 2. Input parameters.

v_f (m·min^{-1})	2	6	10	16	22
f_z (mm)	0.0188	0.0564	0.094	0.1504	0.2068
φ_2 (°)	41.78				
h_m (mm)	0.0125	0.0376	0.0626	0.1002	0.1378

cutting force from it (this part is further processed, and results of the experiment and the calculation of fracture parameters are based on it). The next phase is when the blade leaves the material. This part of measurements is accompanied by a steep drop in forces because the blade is no more pushed to overcome the cutting resistance and the force is stabilized at the values of the so-called passive resistances, caused by aerodynamic losses, friction in the bearings, etc. Values of the passive resistance must be subtracted from the measured values of the torque and the feed force.

Figure 4 shows the linear dependence of the cutting force per one tooth on the rising uncut chip thickness.

Linear regression models have been developed using the QC Expert software (QC-expert AG, Dübendorf, Switzerland). Regression triplet testing, ie testing of data quality, model quality, and quality of the least squares method, was performed on the basis of the Cook–Weisberg test for heteroskedasticity, Jarque–Bera test of normality, Wald test of autocorrelation, and sign test of residues. Table 3 presents the characteristics and parameters of the regression models for individual experiments.

Based on the regression triplet testing, no negative conclusions were made that would affect the credibility of the regression model. Although the linear regression lines have differing parameters, there is no statistically significant difference in quality between the regression equations. The models were validated using the leave-one-out cross-validation (Table 4). Its use is recommended for small data sets. The mean quadratic error of the model cvRMSE (error of the missed case over others, or the training-to-testing error) is an important parameter of the leave-one-out cross-validation. The lower the value, the higher the quality of the model. Based on the mean squared error of the model in the cross-validation and based on the Akaike information criterion, we can conclude that all models are of good quality.

The obtained regression models of the cutting force per tooth, as a function of uncut chip thicknesses, are presented in Fig 4 for processing with the circular saw blade. The cutting force trend was linear, and it was expressed in the form as Eq 7. The average cutting force per one tooth for processing with the circular saw blade, for a tooth position defined by the mean fiber cutting angle $\varphi_2 = 41.72°$, is described as follows:

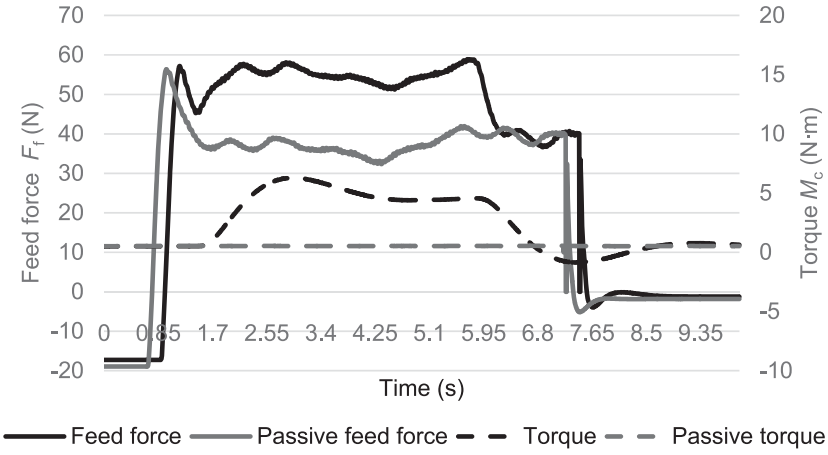

Figure 3. The torque curve and the feed force curve.

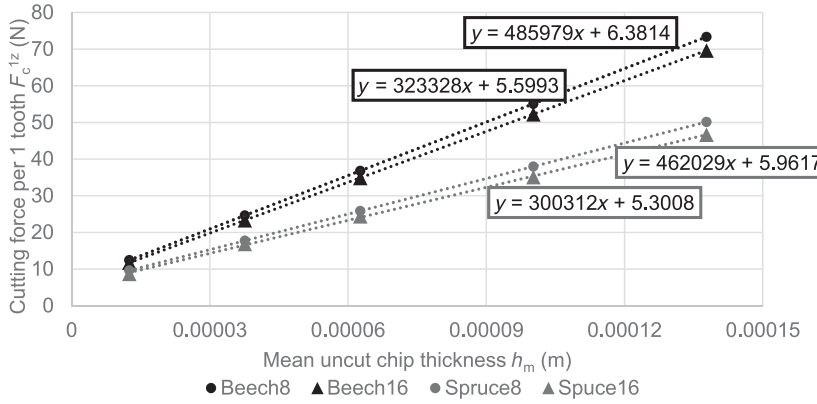

Figure 4. Cutting force per one tooth on mean uncut chip thickness.

$$\text{Beech8} \quad F_c^{1z} = (\varphi_2 = 41.72°) = 485979h_m + 6.3814 \tag{10}$$

$$\text{Beech16} \quad F_c^{1z} = (\varphi_2 = 41.72°) = 462029h_m + 5.9617 \tag{11}$$

$$\text{Spruce8} \quad F_c^{1z} = (\varphi_2 = 41.72°) = 323328h_m + 5.5993 \tag{12}$$

$$\text{Spruce16} \quad F_c^{1z} = (\varphi_2 = 41.72°) = 300312h_m + 5.3008 \tag{13}$$

In the first step, characteristic data were estimated according to Atkins (2005). The toughness $R_{\parallel\perp}$ was determined from the experimental ordinate intercept, where the value of the intercept was 6.3814 (N) for Beech8, 5.9617 (N) for Beech16, 5.5993 (N) for Spruce8, and 5.3008 (N) for Spruce16 (see Eqs 10-13). The value of the slope was determined as 485,979 ($N \cdot m^{-1}$) for Beech8, 462,029 ($N \cdot m^{-1}$) for Beech16, 323,328 ($N \cdot m^{-1}$) for Spruce8, and 300,312 ($N \cdot m^{-1}$) for Spruce16 (Eqs 10-13). Application of the fracture mechanics approach to the sawing processes of both beech and spruce samples on the circular sawing machine yielded fracture toughness $R_{\parallel\perp}\varphi_2 = 41.72°$) and shear yield strength $\tau_{\gamma\parallel\perp}(\varphi_2 = 41.72°)$. Computed values are input data for determination of the fracture parameters (see Table 5) for the axial-perpendicular direction of saw blade cutting.

Comparison of Fracture Features

Ashby et al (1985) focused their research on the relationship between fracture and toughness of

Table 3. Determination of regression model parameters.

	Variable	Estimate	Standard deviation	Conclusion	*p*-value	Lower limit	Upper limit
Beech16	Intercept	5.852665	0.56079	Significant	0.00188	4.06797	7.63737
	Uncut chip thickness	462,356.12	6749.34	Significant	6.8547E-006	440,876.68	483,835.56
Beech8	Intercept	6.381374	0.38315	Significant	0.00047	5.16199	7.60076
	Uncut chip thickness	485,979.92	4611.43	Significant	1.8835E-006	471,304.28	500,655.55
Spruce16	Intercept	7.158473	0.73670	Significant	0.00232	4.813961	9.502985
	Uncut chip thickness	271,138.96	8866.43	Significant	7.6819E-005	242,922.01	299,355.91
Spruce8	Intercept	7.266068	0.58660	Significant	0.001134	5.399238	9.132898
	Uncut chip thickness	298,832.02	7059.94	Significant	2.9021E-005	276,364.12	321,299.91

Table 4. Leave-one-out cross-validation.

	cvR^2	cvRMSE
Beech16	0.9984	0.78
Beech8	0.9976	0.69
Spruce16	0.9961	1.46
Spruce8	0.9965	1.14

different wood species. In particular, they investigated the impact of wood body geometry, density, and direction of crack propagation. Based on their research, it can be concluded that fracture toughness of dry intact wood depends on density, both along and across the fibers. This statement is justified by the fact that samples with a higher density provide greater resistance to crack propagation, thanks to higher concentration of the wood mass (Petterson and Bodig 1983). The same conclusion was published by Leicester (1983), Kretschmann and Nelson (1990), and Gibson and Ashby (1997). Our results (see Table 5) showed the same trend. Fracture toughness of the spruce was lower than that of the beech. For samples with moisture $w = 8\%$, fracture toughness of the spruce was lower by nearly 12%; for samples with moisture $w = 16\%$, it was lower by 11%.

Further influence on fracture toughness is vested to moisture, temperature, and load rate. Kretschmann (2010) argues that there is only restricted information about the influence of moisture on fracture toughness. The available information suggests that fracture toughness is either insensitive to the MC or rises with reducing moisture in the wood. Our findings confirm this claim. Fracture toughness decreased with rising water content in the wood: for beech, the decrease is by 7%; for spruce, the decrease is by 5%. Kretschmann and Green (1996) have established that fracture toughness of the common pine wood reaches maximum values at an MC of $w = 6$-8% and that fracture toughness decreases slightly when the value falls below this moisture level. Nikitin (1966) explains this claim by penetration of water into the crystalline structure of cellulose microfibers. This leads to a decrease in crystallinity and a decrease in fracture toughness afterward. For higher moisture values, the reduced fracture toughness is explained by increased plasticity during crack propagation (Atack et al 1961).

Comparison of shear properties is shown in Table 5, where we can see that the shear yield strength for beech is in all cases higher than that for spruce. If we take into account the fibrous wood structure, we can distinguish different kinds of shear—from the point of view of machining, the shear in the transverse plane (forces act in a radial or tangential direction) approaches best to our method of fracture. This strength of wood is often named fiber cutting or shear yield strength (Požgaj et al 1997). The shear yield strength is 3-4 times higher than the strength parallel to the fibers. The authors provide average shear yield strength values ranging from 20 to 52 MPa (at $w = 12\%$) for different wood species. Results of the shear yield strength calculated on the basis of the performed experiments are as follows: $\tau_{\gamma\parallel\perp} = 57.16$ MPa for Beech8, $\tau_{\gamma\parallel\perp} = 50.61$ MPa for Beech16, $\tau_{\gamma\parallel\perp} = 41.53$ MPa for Spruce8, and $\tau_{\gamma\parallel\perp} = 35.994$ MPa for Spruce16. Mechanical wood features are affected by the anatomical structure, by the factors related to the applied load, or by chemical treatment, and also by the factors related to the environmental conditions where the wood is used (in particular temperature and MC of the wood). If the moisture drops below the FSP, wood volume is decreased. This change in MC also affects the change in mechanical wood features (Kivimaa 1950). We can say in general that water leakage from the cell wall leads

Table 5. Comparison of the parameters input into the newly designed model.

	μ (-)	β_μ (°)	Φ (°)	γ (-)	Q (-)	$\tau_{\gamma\parallel\perp}$ (MPa)	$R_{\parallel\perp}$ (J·m^{-2})
Beech8	0.565	29.486	40.257	1.550	0.656	57.155	1772.611
Beech16	0.661	33.477	38.261	1.598	0.630	50.609	1656.028
Spruce8	0.455	24.471	42.764	1.501	0.694	41.532	1555.361
Spruce16	0.541	28.413	40.793	1.539	0.664	35.994	1472.444

to higher elastic and strength properties. Požgaj et al (1997) claims that if moisture changes by 1% within the bound water range, wood strength will change in average by 3-4%. From Table 5, it is evident that the shear yield strength is always higher for dry wood.

It is necessary to consider both the fracture toughness and the shear yield strength listed in the literature for individual load directions and for the main directions of cutting or crack propagation. However, our measured results represent a combination of these basic directions because sawing was performed in the axial-perpendicular direction of cutting. More detailed comparison of these fracture features with the literature data is, therefore, difficult.

The friction coefficient μ is another important parameter of the model, which affects the friction angle β_μ, the shear plane angle Φ, the shear strain along the shear plane γ and the friction correction coefficient Q_{shear}. Friction coefficient μ values for spruce are lower than those for beech, and similar results have been achieved by Beer (2002). The difference in results between beech and spruce is because of the differing anatomical structure of coniferous and deciduous wood species and differing fiber orientation (McKenzie and Karpovich 1968; Ramananantoandro et al 2007). Aira et al (2014) claims that the resin content of coniferous wood promotes surface slipping, and therefore, the friction coefficient is lower. However, values of the friction coefficient quoted in the literature data usually do not show any difference between softwood and hardwood. According to Glass and Zelinka (2010), the coefficient of friction increases with the rising water content in wood. The same trend is supported by our results: namely, for measurements of both the beech and the spruce samples: the coefficient of friction for Beech16 is $\mu = 0.66$; for Beech8, $\mu = 0.56$; for Spruce16, $\mu = 0.54$; and for Spruce8, $\mu = 0.46$. These results also correspond with the results of Sjödin et al (2008). Orlowski et al (2017) used the friction coefficient $\mu = 0.9$, taken from Glass and Zelinka (2010), in their publication focused on pine sawing.

CONCLUSIONS

Various methods for calculating fracture toughness can be found in the literature. Unfortunately, most of these methods are intended for isotropic materials, or fracture toughness is calculated based on performed fracture tests. Using the newly designed model, it is possible to determine fracture toughness and shear yield strength only on the basis of cutting tests without performing complex fracture tests.

By applying the results obtained in the experiment, we have determined these fracture parameters for the axial-perpendicular direction of cutting using a circular saw blade. This model is, therefore, applicable only for this direction of cutting because both parameters are suitable for the given direction of cutting edge movement and cannot, therefore, be considered constants. Alternatively, these parameters can be converted for two principal directions regarding wood grains, where they can be considered nonvariable features (Orlowski et al 2017; Hlásková et al 2018).

The value of the fracture parameters is affected by the wood species and the wood MC. One representative of coniferous and one representative of deciduous wood species were selected to examine the influence of the wood species. This comparison confirmed the obvious influence of anatomical structures and density on the size effect of fracture parameters. The influence of MC was reflected despite its small change from $w = 16\%$ to $w = 8\%$.

The methodology is applicable in currently used machine tools and tools/accessories (in cases where the rake angle does not exceed 35° and when shear is observed in the cutting zone [Franz 1958]) and to a wide range of materials (wood-based materials and modified industrial materials).

ACKNOWLEDGMENTS

This article is based on research sponsored by the Internal Grant Agency FFWT of Mendel University in Brno. The authors are grateful for support of the project "The Application of Progressive Technologies," which deals with

unconventional material machining (Grant IGA No. LDF_PSV_2016019).

REFERENCES

Aira JR, Arriagaa F, Íñiguez-Gonzáleza G, Crespo J (2014) Static and kinetic friction coefficients of Scots pine (*Pinus sylvestris* L.), parallel and perpendicular to grain direction. Mater Constr 64(315):e030.

Ashby MF, Easterling KE, Harrysson R, Maiti SK (1985) The fracture and toughness of woods. P Roy Soc Lond A Mat 398:261-280.

Atack D, May WD, Morris EL, Sproule RN (1961) The energy of tensile and cleavage fracture of black spruce. Tappi J 44(8):555-567.

Atkins AG (2003) Modelling metal cutting using modern ductile fracture mechanics: Quantitative explanations for some longstanding problems. Int J Mech Sci 45(2): 373-396.

Atkins AG (2005) Toughness and cutting: A new way of simultaneously determining ductile fracture toughness and strength. Eng Fract Mech 72(6):849-860.

Atkins AG (2009) The science and engineering of cutting. The mechanics and process of separating, scratching and puncturing biomaterials, metals and non-metals. Butterworth-Heinemann, Oxford, UK. 432 pp.

Beer P (2002) Wood peeling with new elaborated tools. Roczniki Akademii Rolniczej w Poznaniu. Akademii Rolniczej im. Augusta Cieszkowskiego w Poznaniu, Poznan, Poland. 108 pp.

Csanády E, Magoss E (2013) Mechanics of wood machining. Springer, Berlin, Germany. 202 pp.

Franz NC (1958) An analysis of the wood-cutting process. The University of Michigan Press, Ann Arbor, MI. 166 pp.

Gibson LJ, Ashby MF (1997) Cellular solids: Structure and properties. Cambridge University Press, Cambridge, UK.

Glass SV, Zelinka SL (2010) Moisture relations and physical properties of wood. Pages 4/1-4/19 *in* Wood handbook—Wood as an engineering material. General Technical Report FPL-GTR-190. U.S. Department of Agriculture, Forest Service, Forest Products Laboratory, Madison, WI.

Hlásková L, Orlowski KA, Kopecký Z, Jedinák M (2015) Sawing processes as a way of determining fracture toughness and shear yield stresses of wood. BioResources 10(3):5381-5394.

Hlásková L, Orlowski KA, Kopecký Z, Sviták M, Ochrymiuk T (2018) Fracture toughness and shear yield strength determination for two selected species of central European provenance. BioResources 13(3):6171-6186.

Kivimaa E (1950) The cutting force in woodworking. Report No. 18. The State Institute of Technical Research, Helsinki, Finland. 103 pp.

Kopecký Z, Hlásková L, Orlowski K (2014) An innovative approach to prediction energetic effects of wood cutting process with circular-saw blades. Wood Res-Slovakia 59(5):827-834.

Kopecký Z, Rousek M (2012) Impact of dominant vibrations on noise level of dimension circular sawblades. Wood Res-Slovakia 57(1):151-160.

Kowaluk G (2007) Application of the theory of work of cutting distribution in milling. Electron J Pol Agric Univ 10(3):1-8.

Kowaluk G, Dziurka D, Beer P, Sinn G, Stanzl-Tschegg SE (2004) Influence of ammonia on particleboard properties. Pages 459-465 *in* Proc 2nd International Symposium on Wood Machining, 5-7 July 2004, Vienna, Austria.

Kretschmann DE (2010) Mechanical properties of wood. Pages 5/1-5/46 *in* Wood handbook—Wood as an engineering material. General Technical Report FPL-GTR-190. U.S. Department of Agriculture, Forest Service, Forest Products Laboratory, Madison, WI.

Kretschmann DE, Green DW (1996) Modeling moisture content-mechanical property relationships for clear southern pine. Wood Fiber Sci 28(3):320-337.

Kretschmann DE, Nelson WJ (1990) The effect of moisture content on mode I fracture toughness in southern pine. Pages 274-303 *in* Proc IUFRO S5.02 Timber Eng, St. John, New Brunswick and Montreal, Quebec, Canada, July/August 1990.

Laternser R, Gänser H, Taenzer L, Hartmaier A (2003) Chip formation in cellular materials. J Eng Mater Technol 125(1):44-49.

Leicester RH (1983) The fracture strength of wood. Workshop on Timber Engineering, Melbourne, Australia, 2-20 May 1983. 11:1-24.

McKenzie W, Karpovich H (1968) The frictional behaviour of wood. Wood Sci Technol 2:139-152.

Nikitin NI (1966) The chemistry of cellulose and wood. Israel Program for Scientific Translations, Jerusalem, Israel. 691 pp.

Orlowski K (2007) Experimental studies on specific cutting resistance while cutting with narrow-kerf saws. Adv Manuf Sci Technol 31(1):49-63.

Orlowski KA, Atkins A (2007) Determination of the cutting power of the sawing process using both preliminary sawing data and modern fracture mechanics. Pages 171-174 *in* Proc Third International Symposium on Wood Machining. Fracture Mechanics and Micromechanics of Wood and Wood Composites with Regard to Wood Machining, May 21-23, Lausanne, Switzerland.

Orlowski KA, Pałubicki B (2009) Recent progress in research on the cutting process of wood. A review COST Action E35 2004-2008: Wood machining-micromechanics and fracture. Holzforschung 63(2):181-185.

Orlowski K, Ochrymiuk T, Atkins A, Chuchala D (2013) Application of fracture mechanics for energetic effects predictions while wood sawing. Wood Sci Technol 47(5):949-963.

Orlowski KA, Ochrymiuk T, Sandak J, Sandak A (2017) Estimation of fracture toughness and shear yield stress of orthotropic materials in cutting with rotating tools. Eng Fract Mech 178:433-444.

Patel Y, Blackman BRK, Williams JG (2009) Measuring fracture toughness from machining tests. P I Mech Eng C-J Mec 223(12):2861-2869.

Petterson RW, Bodig J (1983) Prediction of fracture toughness of conifers. Wood Fiber Sci 15(4):302-316.

Požgaj A, Chovanec D, Kurjatko S, Babiak M (1997) Structure and properties of wood. Príroda a.s., Bratislava, Slovakia. 486 pp. [In Slovak].

Ramananantoandro T, Eyma F, Paris JY, Denape J (2007) Linear measurement of friction parameters on oak pedunculate as related to wood ligneous plane. Pages 93-99 *in* P Navi and A Guidoum, eds. Proc Third International Symposium on Wood Machining, May 21-23, 2007, Switzerland.

Reuleaux F (1900) About the Taylor tule white tool steel. Society for the promotion of trade diligence in Prussia. Sitzungsberichete 79(1):179-220.

Sjödin J, Serrano E, Enquist B (2008) An experimental and numerical study of the effect of friction is single dowel joints. Holz Roh-Werkst 66:363-372.

Williams JG (1998) Friction and plasticity effects in wedge splitting and cutting fracture tests. J Mater Sci 33(22): 5351-5357.

Williams JG, Patel Y, Blackman BRK (2010) A fracture mechanics analysis of cutting and machining. Eng Fract Mech 77(2):293-308.

Wyeth DJ, Goli G, Atkins AG (2009) Fracture toughness, chip types and mechanincs of cutting wood. A review COST Action E35 2004-2008: Wood machining–micromechanics and fracture. Holzforschung 63(2): 168-180.